

Photoinduced electron transfer of $[\text{Ru}(\text{bpy})_2(4,4'\text{-dcbpy})]^{2+}$ with electron donors

XIE, Pu-Hui(谢普会) ZHANG, Lian-Qi(张联齐) HOU, Yuan-Jun(侯原军)

ZHANG, Bao-Wen*(张宝文) CAO, Yi*(曹怡)

Institute of Photographic Chemistry, Chinese Academy of Sciences, Beijing 100101, China

WU, Fang(吴芳) TIAN, Wen-Jing(田文晶) SHEN, Jia-Cong(沈家骢)

Key Laboratory for Supramolecular Structure and Spectroscopy, Jilin University, Changchun, Jilin 130023, China

Emission quenching of $[\text{Ru}(\text{bpy})_2(4,4'\text{-dcbpy})](\text{PF}_6)_2$ (**1**) by benzenamine, 4-[2-[5-[4-[4-dimethylamino]phenyl]-4,5-dihydro-1-phenyl-1H-pyrazol-3-yl]-ethenyl]-*N,N*-dimethyl (**2**) or 1,5-diphenyl-3-(2-phenothiazine)-2-pyrazoline (**3**) was observed. Measurements of the emission decay of **1** before and after addition of **2** or **3** by single photon counting technique confirmed the observations. The emission quenching of **1** by **2** or **3** was submitted to Stern-Volmer equation. It was calculated that the quenching rate constants (k_q) are $5.5 \times 10^9 (\text{mol/L})^{-1} \text{s}^{-1}$ for **2** and $4.0 \times 10^9 (\text{mol/L})^{-1} \text{s}^{-1}$ for **3**, respectively. These results indicated a character of dynamic quenching process. The singlet-state of **2** or **3** was also quenched by **1**. The quenching behaviors did not conform to the Stern-Volmer equation and involved both static and dynamic quenching processes. The apparent quenching rate constant (k_{app}) was calculated to be $3 \times 10^9 (\text{mol/L})^{-1}$ for the interaction of excited **2** with **1**, and $1.2 \times 10^9 (\text{mol/L})^{-1}$ for that of excited **3** with **1**.

Keywords Ruthenium complexes, pyrazoline compounds, electron-transfer, dynamic quenching

Introduction

Since Gratzel *et al.* reported highly efficient solar cells ($\eta_{\text{sun}} = 10\%$) based on a porous TiO_2 semiconductor electrode sensitized by Ru complex,¹ dye sensitization of wide bandgap semiconductors has been investigated from the standpoint of simple production of highly efficient solar cells. Sensitizers such as Ru(II) complexes have been employed to increase the charge carrier generation efficiently and to broaden the photoaction spectrum. And

nearly quantitative conversion of light into electric current is demonstrated for photoelectrochemical cells with nanocrystalline TiO_2 electrodes coated with an appropriate Ru(II) complex. The large conversion efficiency is explained by the efficient vectorial electron injection from the photoexcited state of the dye into the conduction band of semiconductor particles. This produces an interfacial charge pair with the electron in TiO_2 and the hole localized on the Ru center. Because light absorption is more clearly separated from the charge carrier transport, the dye-sensitized photoelectrochemical solar cells differ from the conventional solar cells. In the case of sensitized cells, when a dye molecule absorbs a photon, and the excited dye molecule injects an electron into the conduction band of the semiconductor, a photocurrent can be generated. But in a regenerate solar cell, electron transfer from a redox species in the solution must recycle the dye.

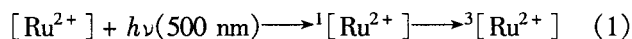
To provide sustainable energy sources for the future, considerable efforts must be made to reproduce artificially the light-induced charge separation reactions of solar cells. $[\text{Ru}(\text{bpy})_2(4,4'\text{-dcbpy})]^{2+}$ and related complexes were used widely in this area in view of their possible application in solar energy conversion systems. Such molecules possess good qualities, such as photostability, high extinction coefficients in the visible region, relatively long-lived excited states, and ability to interact with semiconductor surfaces.²

In this paper, we report two new electron donor-acceptor systems of **1** and **2** or **3**. In such systems, photoex-

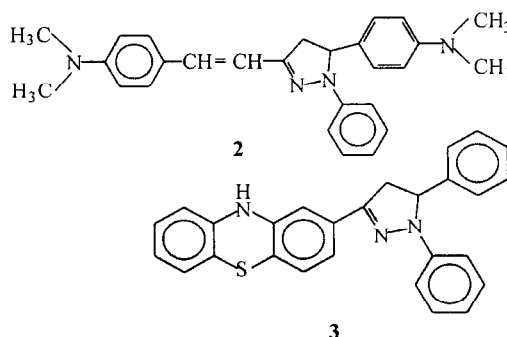
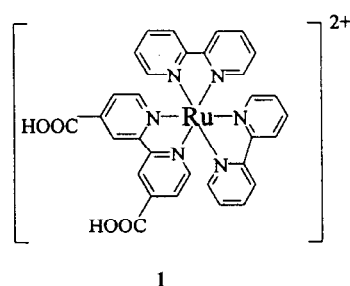
Received March 23, 1999; accepted November 16, 1999.

Project (Nos. 29971031, 29733100) supported by the National Natural Science Foundation of China.

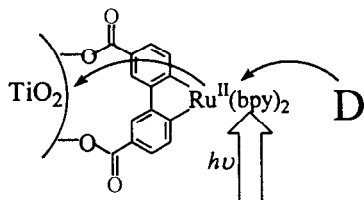
citation of ruthenium polypyridyl complexes such as **1** generated a singlet metal-to ligand charge-transfer state ($^1\text{MLCT}$), which underwent a rapid, highly efficient intersystem crossing ($\varphi_{\text{isc}} \approx 1$) to a manifold of closely-spaced triplet states ($^3\text{MLCT}$), a relatively long-lived excited state (see Eq. 1):



2 and **3** (Scheme 1) were selected as electron donors to provide an electron to $^3[\text{Ru}^{2+}]$ by formation of $[\text{Ru}]^{\dagger}$



Scheme 1



Experimental

Materials

N,N-Dimethyl formamide (DMF) was purified by distillation after being dried with MgSO_4 for 24 h. All other solvents and chemicals were of the purest quality and used as purchased.

2,2'-Bipyridine-4,4'-dicarboxylic acid was prepared according to literature procedures.³ Bis(2,2'-bipyridine)-(2,2'-bipyridine-4,4'-dicarboxylic acid) ruthenium(II)-(PF_6)₂, $[\text{Ru}(\text{bpy})_2(4,4'\text{-dcbpy})](\text{PF}_6)_2$ (**1**) was prepared by the method reported in the literature.⁴ Compounds **2** and **3** were synthesized by the method described in the literature.^{5,6}

Millimolar solutions of the compounds were prepared

and $[\text{donor}]^{\dagger}$ and the emission of **1** was quenched correspondingly as Scheme 1. Excited **2** or **3** can give electron to the ground-state of **1** and the fluorescence of **2** or **3** was quenched. Due to their high melting point, **2** or **3** may serve as organic hole-transport material in solid-state solar cells, in which they can prevent crystallization of the organic material. These materials could act as charge propagating medium in dye sensitized solid state solar cells and provide much prospect for overcoming the disadvantages of liquid-junction cells.

in 0.1 mol/L acetonitrile solutions of tetra-*n*-butylammonium tetrafluoroborate in cyclic voltammetry measurements. The acetonitrile was freshly distilled over P_2O_5 . The solutions were deaerated by purging with N_2 over 25 min.

Apparatus

Absorption spectra were taken with Hitachi U-2001 spectrophotometer and steady-state emission spectra were recorded on Perkin-Elmer Ls-05 fluorimeter equipped with a computer for data acquisition, storage, and manipulation. The emission lifetimes were measured at room temperature with the single photon counting technique on a Horiba NAES-1100 time-resolved emission spectrophotometer. Lifetime analysis was made with the deconvolution program. Cyclic voltammetry measurements were made with HPD-IA equipment. All voltammograms were recorded under nitrogen atmosphere with a Pt microcylinder working electrode, a Pt wire auxiliary electrode, and a standard calomel reference electrode. Cyclic voltammetry of the ferrocene/ferrocenium redox couple was performed after each experiment to calibrate the pseudo-reference electrode.

Results and discussion

Electrochemistry and thermodynamic discussion

Redox potentials for the compounds in CH₃CN are obtained by cyclic voltammetry. The results are listed in Table 1. The oxidation of **1** corresponds to removal of an electron from d orbital of Ru(II) to give Ru(III). The reduction of **1** corresponds to reduction of the 4,4'-dcbpy ligand in the mixed [Ru(bpy)₂L]²⁺.

The free energy changes (ΔG) for the primary photoinduced electron transfer process could be calculated using Rehm-Weller equation:⁷

$$\Delta G = E_{\text{ox}}(\text{D}) - E_{\text{red}}(\text{A}) - E_{0,0} - C \quad (2)$$

where $E_{\text{ox}}(\text{D})$ is the oxidation potential of donor, $E_{\text{red}}(\text{A})$ is the reduction potential of acceptor, $E_{0,0}$ is the excited state energy of the excited compound, C is the columbic energy of $\text{D}^{\ddagger} \text{A}^{\ddagger}$, which can usually be regarded as 0.06 eV or 5.8 kJ/mol in polar solvents.⁸

Table 1 shows that MLCT excited energy of **1** is lower than the singlet energies of **2** or **3**, $\Delta E < 0$. So when **1** is excited, there will be no energy transfer between **1** and **2** or **3**. The free energy changes (ΔG) of forward electron transfer for the two systems are -0.463 eV and -0.312 eV, respectively, indicating that the electron transfer process in the above two systems is feasible. When **2** or **3** is excited, the electron transfer processes can occur sponta-

neously from **2** or **3** to **1**, with $\Delta G = -1.16$ eV and $\Delta G = -0.87$ eV, respectively. Furthermore, the energy transfer may also due to overlap between the absorption spectrum **1** and the fluorescence spectrum of **2** or **3**.

Table 1 Excitation energy values and cyclic voltammetry data for model compounds in CH₃CN^a

Compound	^b $E_{0,0}$ (eV)	^c E_{ox} (V)	E_{red} (V)
1	2.255 (550 nm)	1.266	-1.50
2	2.953 (420 nm)	0.352	0.526 0.874
3	2.818 (440 nm)	0.503	0.763

^a All potentials for 10⁻³ mol/L compounds with 0.1 mol/L tetra-*n*-butylammonium tetrafluoroborate as supporting electrolyte. Volt *vs.* SCE, error in potentials was ± 0.002 V, $T = 25 \pm 1$ °C, scan rate = 100 mV/S. ^b The values of $E_{0,0}$ were obtained from the absorption spectra at 298 K. It should be noted that $E_{0,0}$ can not be rigorously determined, because of the approximations required in the spectral modeling of the lower frequency modes and the lack of spectral resolution. ^c Mean of cathodic and anodic half-wave potential values.

Absorption spectra

Fig. 1a shows the absorption spectra of **1**, **2** and of the mixture of **1** and **2** (curve 3) in acetone solution. It can be seen that curve 3 is nearly identical to the sum of **1** (curve 1) and **2** (curve 2) in strength and shape. The similar phenomenon of absorption spectra was also observed in the case of **1** and **3** system. It is obvious that there is no interaction of **1** with **2** or **3** in the ground state.

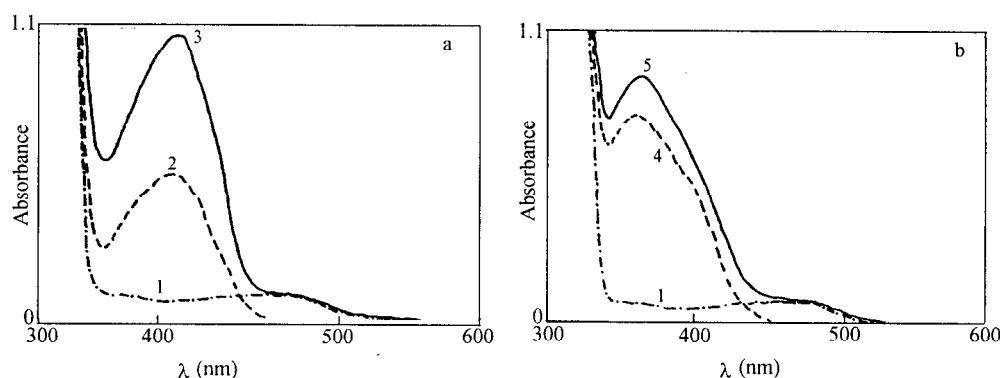


Fig. 1 (a) Absorption spectra of **1** (1×10^{-5} mol/L) (curve 1), **2** (2×10^{-5} mol/L) (curve 2), the mixture of (1:1.5) **1** and **2** (curve 3) in acetone solutions; (b) Absorption spectra of **1** (1×10^{-5} mol/L) (curve 1), **3** (2×10^{-5} mol/L) (curve 4), the mixture of (1:1) **1** and **3** (curve 5) in acetone solutions.

Emission quenching of **1** by **2** or **3**

A series of **1** and **2** mixtures in acetone solution were prepared. The concentration of **1** is 2.7×10^{-4} mol/L, that of **2** is in the range of 0 to 1×10^{-3} mol/L. The excitation wavelength is 500 nm, where **2** has no absorption. Upon excitation of **1**, an emission spectrum appears in the region of 550 to 750 nm, which comes from the excited MLCT(³MLCT). Upon addition of different concentrations of **2**, the emission intensity of **1** is quenched markedly as shown in Fig. 2a. 80% of its original emission intensity is diminished at 1×10^{-3} mol/L of **2**. The emission peaks are almost not shifted. The quenching mechanism involves photoinduced electron transfer process between the ³MLCT of **1** to the ground state of **2** as Eq. 3 and Scheme 2.

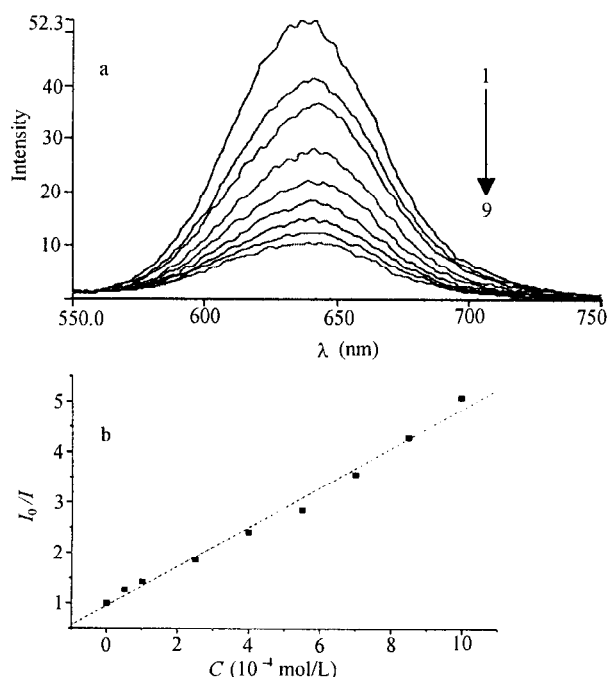
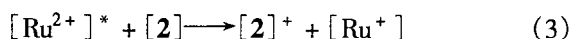


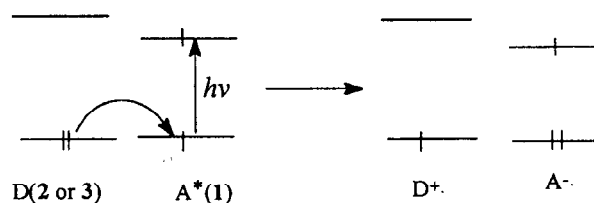
Fig. 2 (a) Emission spectra of **1** (2.7×10^{-4} mol/L) in acetone solution with various concentrations of **2**: (1) 0, (2) 5×10^{-5} mol/L, (3) 1×10^{-4} mol/L, (4) 2.5×10^{-4} mol/L, (5) 4×10^{-4} mol/L, (6) 5.5×10^{-4} mol/L, (7) 7×10^{-4} mol/L, (8) 8.5×10^{-4} mol/L, (9) 1×10^{-3} mol/L ($\lambda_{\text{ex}} = 500$ nm); (b) Stern-Volmer curve (I_0/I vs $[Q]$).

Table 2 single-exponential-fit parameters for observed emission decay of **1** in the absence and presence of **2** or **3** ($\lambda_{\text{ex}} = 500$ nm; $\lambda_{\text{em}} = 640$ nm) and values of calculated K_q

solutions	τ (ns)	χ^2 (Chi square)	Calculated k_q
1 (2.7×10^{-4} mol/L)	734	1.39	—
1 in 2 (1×10^{-3} mol/L)	144	1.41	5.5×10^9
1 in 3 (1×10^{-3} mol/L)	185	1.18	4.0×10^9

Fig. 2b shows that the emission quenching follows Stern-Volmer equation.^{9,10} I_0/I shows linear dependence on the concentrations of **2**. The slope of the straight line affords $k_q\tau_0 = 3.9 \times 10^3$ (mol/L)⁻¹ by linear fit, the linear relative coefficient (R) is 0.99505, showing good linear relation.

Scheme 2 Simplified view of a model for electron transfer to an excited acceptor



The emission quenching of **1** is also confirmed by measurements of the time-resolved intensity of its emission as shown in Table 2, which exhibits the decay results of **1** at 640 nm in the absence and presence of **2** or **3**. Table 2 contains pertinent fitting parameters, from which shortened decay times of **1** after addition of **2** or **3** are observed. As the value of τ_0/τ equals to that of I_0/I within the experimental error for excited **1** by addition of **2**, the emission quenching from **2** to excited **1** is a dynamic quenching character. According to Stern-Volmer equation (Eq. 4)

$$\tau_0/\tau = 1 + k_q\tau_0C_q$$
 (4)

where k_q is bimolecular constant of quenching rate, τ_0 and τ are luminescence lifetimes in the absence and presence of a quencher respectively, C_q is the quencher concentration. Since $\tau_0 = 734$ ns, so the observed rate constant is calculated to be $k_q^{\text{obs}} = 5.5 \times 10^9$ (mol/L)⁻¹s⁻¹ for **2** as an electron donor.

Similar emission quenching experiment of **1** by **3** was also carried out as shown in Fig. 3a. The k_q^{obs} is derived as 4.0×10^9 (mol/L)⁻¹s⁻¹ as shown in Table 2, R is

given to be 0.99666. And the quenching character is also a dynamic process by comparing the value of τ/τ_0 with that of I/I_0 .

The efficiency of electron transfer Φ_{ET} can be calculated using Eq. 5:

$$\Phi_{ET} = 1 - \tau/\tau_0 \quad (5)$$

which gives the value of 0.8 for ground state **2** and the excited state Ru complex, that of 0.75 for excited **1** and the ground state **3**. So the quenching ability of **2** is slightly larger than **3** in the same condition, which can also be verified by comparing the first oxidation potentials of **2** and **3**. The lower the oxidation potential, the larger the quenching ability.

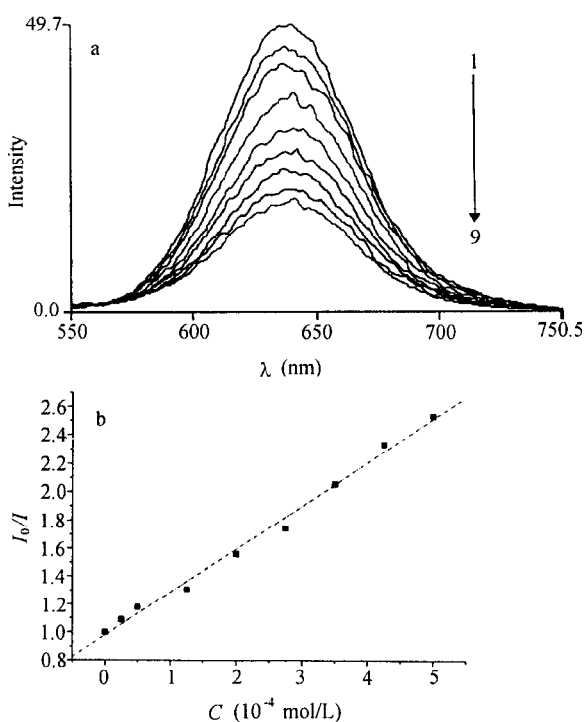


Fig. 3 (a) Emission spectra of **1** (2.7×10^{-4} mol/L) in acetone with various concentrations of **3**: (1) 0, (2) 2.5×10^{-5} mol/L, (3) 5×10^{-5} mol/L, (4) 1.25×10^{-4} mol/L, (5) 2×10^{-4} mol/L, (6) 2.75×10^{-4} mol/L, (7) 3.5×10^{-4} mol/L, (8) 4.25×10^{-4} mol/L, (9) 5×10^{-4} mol/L ($\lambda_{ex} = 500$ nm); (b) Stern-Volmer curve (I_0/I vs. $[Q]$).

Fluorescence quenching of **2** or **3** by **1**

When **2** is excited at 360 nm, it emits in the region of 420 to 600 nm with a maximum emission peak at 458

nm as shown in Fig. 4a. With the addition of **1**, the fluorescence intensity of **2** is obviously decreased. 4.4×10^{-5} mol/L of **1** quenches 80% of the original intensity of **2**. And the fluorescence peaks show gradually red-shifts to about 510 nm. Fig. 4b shows the Stern-Volmer plot for the fluorescence quenching of **2** with different concentrations of **1**. Increasing concentrations enhances the fluorescence quenching. The emission quenching data do not conform the Stern-Volmer equation. I_0/I exhibits nonlinear dependence on the concentrations of **1**. This implies that the fluorescence quenching of **2** by **1** involves both dynamic and static mechanisms. The apparent quenching rate constant k_{app} is 3×10^9 (mol/L) $^{-1}$ by calculation.

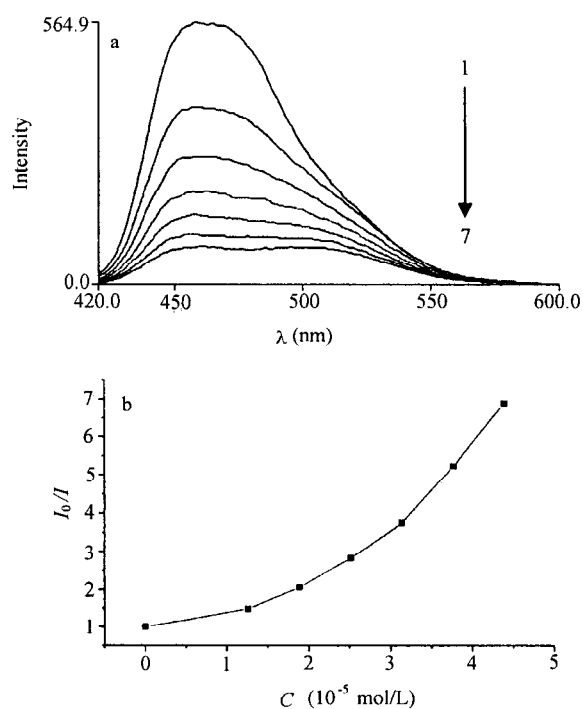
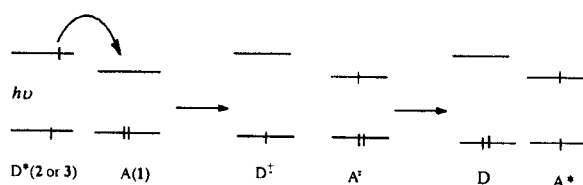


Fig. 4 (a) Fluorescence spectra of **2** (1×10^{-6} mol/L) by addition of various concentrations of **1**. $\lambda_{ex} = 380$ nm): (1) 0, (2) 1.26×10^{-5} mol/L, (3) 1.89×10^{-5} mol/L, (4) 2.52×10^{-5} mol/L, (5) 3.14×10^{-5} mol/L, (6) 3.78×10^{-5} mol/L, (7) 4.40×10^{-5} mol/L; (b) Stern-Volmer curve (I_0/I vs. $[Q]$).

Similar experimental phenomenon is observed that **1** could quench the fluorescence of **3**, the apparent quenching rate constant k_{app} is calculated to be 1.2×10^9 (mol/L) $^{-1}$. This shows that the donor (**2** or **3**) can give an excited electron to acceptor (**1**) (Scheme 3). As $E_D > E_A$,

and the fluorescence band of the donor (**2** or **3**) overlaps the absorption band of acceptor (**1**), the energy can be partly transferred to **1** from excited **2** or **3**.

Scheme 3 Electron transfer and energy transfer from an excited donor



Controllable experiment was carried out to verify the possibility of energy transfer. When 4.5×10^{-5} mol/L of **1** was excited at 360 nm, there are two emission bands between 420 nm and 700 nm, with two maximum peaks (*ca.* 510 nm assigned to $\pi \rightarrow \pi^*$ and 640 nm attributed to $^3\text{MLCT}$ as shown in Fig. 5), the emission intensity of $^3\text{MLCT}$ is very weak. Because there are no emission around 640 nm by addition of **1**, and the emission peaks of **2** are shifted to *ca.* 510 nm gradually, the excited state of **2** can transfer its part energy to **1**, thus leading to $\pi \rightarrow \pi^*$ transition as shown in Fig. 4a.

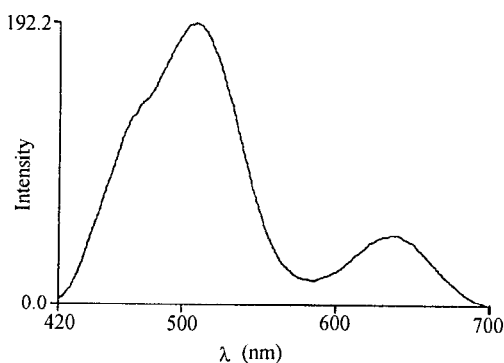


Fig. 5 Emission spectrum of $[\text{Ru}(\text{bpy})_2(4,4'\text{-dcbpy})]-(\text{PF}_6)_2$ (**1**, 5×10^{-5} mol/L) in acetone solution ($\lambda_{\text{ex}} = 360$ nm).

The excited Ru complex and the singlet state of **2** differ in energy by 0.7 eV, so that the energy transfer from singlet state of **2** to Ru complex is thermodynamically

favorable. But it is obvious that the contribution of the electron transfer is more than that of energy transfer. The energy of the excited **2** consumes mainly through the way of the electron transfer to **1**, while the energy transfer is the minor way.

The above experimental results indicate that **2** and **3** may act as solid hole conducting materials in ruthenium complex of dye-sensitized solid solar cells.

Conclusion

The interactions of **1** with **2** or **3** in acetone solution are investigated. The emission quenching is also carried out by time-resolved emission decay of **1** before and after addition of **2** or **3**. The quenching process involves an electron transfer mechanism, in which **2** or **3** acts as electron donor. The measured quenching rate constants are 5.5×10^9 (mol/L) $^{-1}$ and 4.0×10^9 (mol/L) $^{-1}$ of **1** by **2** or **3**, respectively. The quenching processes for excited **2** or **3** by **1** involve both electron transfer and energy transfer processes with apparent quenching rate constant of 3×10^9 (mol/L) $^{-1}$ and 1.2×10^9 (mol/L) $^{-1}$, respectively. These studies may provide a novel idea for the study of solid solar cells with these electron donors as hole transport materials.

References

- O'Regan, B.; Gratzel, M., *Nature*, **353**, 737 (1991).
- Fessenden, R.W.; Kamat, P.V., *J. Phys. Chem.*, **69**, 12902(1995).
- Sprintschnik, G.; Sprinschnik, H.W.; Kirsch, P.P.; Whitten, D.G., *J. Am. Chem. Soc.*, **98**, 4947(1976).
- Anderson, S.; Seddon, K.R.; Constable, E.C.; Baggott, J.E.; Pilling M.J., *J. Chem. Soc., Dalton Trans.*, **2247**(1985).
- Rivett, D.E.; Roseverar, J.; Wilshire, J.F.K., *Aust. J. Chem.*, **32**, 1601(1979).
- Sandler, S.R.; Tsou, K.C., *J. Chem. Phys.*, **39**, 1062 (1963).
- Kararnos, G.J.; Tarro, N.J., *Chem. Rev.*, **86**, 401 (1986).
- Fankner, L.R.; Tachikawa, H.; Bard, A.J., *J. Am. Chem. Soc.*, **94**, 691(1972).
- Stern, O.; Vollmer, M., *Phys. Z.*, **20**, 183(1919).
- Wagner, P.J., *Creation and Detection of the Excited State*, Vol. 1, Pt. A, Manel Dekker, New York, 1971, p. 173.